13

Monte Carlo Simulation of Electron Dynamics in Doped Semiconductors Driven by Electric Fields: Harmonic Generation, Hot-Carrier Noise and Spin Relaxation

Dominique Persano Adorno
Dipartimento di Fisica e Tecnologie Relative,
Università di Palermo and CNISM-INFM,
Viale delle Scienze, edificio 18, I-90128 Palermo
Italy

1. Introduction

In solid state electronics the miniaturization of integrated circuits implies that, even at moderate applied voltages, the components can be exposed to very intense electric fields. Advances in electronics push the devices to operate also under cyclostationary conditions, i.e. under large-signal and time-periodic conditions. A main consequence of this fact is that circuits exhibit a strongly nonlinear behavior. Furthermore, semiconductor based devices are always imbedded into a noisy environment that could strongly affect their performance, setting the lower limit for signal detection in electronic circuits. For this reason, to fully understand the complex scenario of the nonlinear phenomena involved in the devices response, an analysis of the electron dynamics in low-doped semiconductors far from equilibrium conditions is very important. Semiconductor spintronics offers a possible direction towards the development of hybrid devices that could perform logic operations, communication and storage, within the same material technology: electron spin could be used to store information, which could be transferred as attached to mobile carriers and, finally, detected. Despite these advantages, for the operability of prospective spintronic devices, the features of spin relaxation at relatively high temperatures, jointly with the influence of transport conditions, should be firstly well understood.
This chapter reviews recent results obtained by using a three dimensional semiclassical multivalleys Monte Carlo code to simulate the nonlinear carrier dynamics in low-doped GaAs bulks (Persano Adorno et al., 2009a; Persano Adorno, 2010; Spezia et al., 2010). The aim is to discuss and clarify the most relevant findings obtained by the investigation of: (a) the harmonic generation process and (b) the spectral density of the electron velocity fluctuations in the presence of intense sub-terahertz electric fields;(c) the influence of temperature and transport conditions on the electron spin relaxation.
Since Monte Carlo approach includes, at a microscopic level, all the sources of the nonlinearities (hot carriers, velocity overshoot, intervalley transfer, etc.) which take place in electronic devices operating under large-signal conditions, it allows to study harmonic

generation in the presence of far-infrared fields. Research along this line is motivated both by the desire to understand the response of doped semiconductors to high-power submillimeter radiation and by the possibility of applications to frequency conversion of coherent radiation in the THz frequency region, where other conventional techniques are ineffective or difficult to realize. In the first part of the chapter, the results of the analysis of the polarization of the generated harmonics are reported (Persano Adorno, 2010). In particular, the polarization obtained from the mixing of an oscillating electric field and a static field is compared with that obtained in the presence of two ciclostationary fields, having an integer ratio between the two frequencies. The findings show that the strength and the polarization of the mixed-fields emission exhibit a strong dependence on the angle between the orientation of the two fields. Unusual polarization features of the generated harmonics are found and discussed.

Recently, studies concerning the constructive aspects of noise and fluctuations in different non-linear systems have shown that the addition of external noise to systems with an intrinsic noise may result in a less noisy response. In the central part of the chapter the attention is focused on the calculation of the modifications of the electronic noise spectra caused by the addition of an external correlated noise source. Numerical results show that, under specific conditions, the presence of a fluctuating component, added to a driving oscillating electric field, can reduce the total noise power. Furthermore, a non-linear behavior of the spectral density with the noise intensity is found. Critically depending on the external noise correlation time, the system benefits from the constructive interplay between the random fluctuating electric field and the intrinsic noise of the system. This is a relevant example of noise enhanced stability (NES) in semiconductor systems (Persano Adorno et al., 2009a).

The last part of the chapter is dedicated to the investigation of the influence of temperature and transport conditions on the electron spin depolarization, making use of a Monte Carlo code which includes the precession description of the spin polarization vector. In order to make spintronics a viable prospective technology it needs to find out the best conditions to achieve long spin relaxation times and/or spin diffusion lengths in semiconductor materials. Electron spin depolarization lengths and times show a nonmonotonic dependence on both the lattice temperature and the electric field amplitude (Spezia et al., 2010). Both parameters appear to be fundamental for the design and fabrication of spintronic devices.

2. Monte Carlo approach

The correct theoretical description of a semiconductor device can be obtained by self-consistently solving the Boltzmann transport equation, or the quantum mechanical equivalent of it, and the Maxwell field equations. In the presence of high amplitude driving fields or under cyclostationary conditions, no analytical solution of the Boltzmann equation is known. Approximate solutions can be obtained within drift-diffusion or hydrodynamic models, but the validity of these models is very limited. It becomes necessary to perform a numerical simulation of the process and Monte Carlo approach represents one of the most powerful methods to simulate the transport properties in semiconductor devices, beyond the quasi-equilibrium approximations. This technique, representing a space-time continuous solution of the field and transport equations, is suitable for studying both the steady state and the dynamic characteristics of the devices. Owing to its flexibility, Monte Carlo method presents the remarkable advantage of giving a detailed description of the particle motion in the semiconductor, by taking into account the main details of band structure, scattering processes and heating effects, specific device design and material parameters. It allows to obtain important electron dynamics information, such as the average velocity,

temperature, current density, etc., directly without the need of calculating first the electron distribution function. The time interval between two collisions (time of free flight), the scattering mechanisms, the collisional angle, and all parameters of the problem are chosen in a stochastic way, making a mapping between the probability density of the given microscopic process and a uniform distribution of random numbers.

In our code the conduction bands of GaAs are represented by the Γ-valley, by four equivalent L valleys and three *X*-valleys. The algorithm includes: (i) the intravalley scattering with acoustic phonons, ionized impurities, acoustic piezoelectric phonons, polar optical phonons, and for the the L-valleys also the scattering with optical nonpolar phonons; (ii) the intervalley scattering with the optical nonpolar phonons. Here all simulations refer to a GaAs bulk with a free electron concentration $n = 10^{13}$ cm^{-3}. With this value of impurity density and for the range of investigated temperatures ($80<T<300$ K) the Fermi temperature is much smaller than the electron temperature and degeneracy does not play any important role. We assume that all donors are ionized and that the free electron concentration is equal to the doping concentration. The complete set of n-type GaAs parameters used in the calculations is listed in Ref. (Persano Adorno et al., 2000). The scattering probabilities are calculated by the Fermi Golden Rule and assumed to be both field and spin independent; accordingly, the influence of the external fields is only indirect through the field-modified electron velocities. Nonlinear interactions of the field with the lattice and bound carriers are neglected. We also neglect electron-electron interactions and consider electrons to be independent (Kiselev & Kim, 2000). The spin polarization vector is included into the Monte Carlo algorithm and calculated for each free carrier, by taking into account the scattering-induced deviations of precession vector suffered after each collision.

The MC simulation is carried out by: (a) setting up the initial conditions of the system by giving to the electrons spin polarization, random momentum direction and kinetic energies with Maxwellian distribution depending on the lattice temperature; (b) determining the free flight time of each electron and updating the energy, the momentum and the spin polarization vector at the end of the free flight; (c) selecting a scattering process for each electron; (d) calculating the new value of energy (in case of inelastic scattering) and the scattering angles of each electron. The simulation continues from point (b). At fixed sampling time steps, small enough to properly update the particle motion, the average values of the physical quantities of interest, such as temperature, average electron velocity, spin polarization vector, are calculated.

3. Harmonic generation process in the presence of intense sub-terahertz electric fields

3.1 A short introduction to the problem

The comprehension of the harmonic generation process in solid state nonlinear materials under the influence of far-infrared fields is important in perspective to use upconversion to create coherent sources of terahertz radiation and/or new devices for microwave and terahertz optics and electronics (Mikhailov, 2008; 2009). With this aim the process of harmonic emission arising from the interaction of semiconductor structures with intense radiation fields, having frequencies in the sub-THz range, has been both experimentally (Brazis et al., 1998; 2000; Moreau et al., 1999; Urban et al., 1995; 1996) and theoretically (Persano Adorno et al., 2000; 2001; 2004; 2007a;b; Shiktorov et al., 2002a;b; 2003a) widely investigated. Moreover, this field of research represents an useful tool for the general understanding of several features of the highly non linear processes of carrier transport in low-doped semiconductors. The basic

physical mechanism yielding harmonic generation in these materials, under cyclostationary conditions, is provided by carrier heating via scattering mechanisms. Indeed, the onset of a scattering mechanism usually results in a kink in the static velocity-field relation at some threshold electric field, corresponding to a characteristic energy (optical phonon energy, energy gap between the lower and upper valleys). Such kinks create a nonlinearity in the velocity-field relation which is responsible for velocity harmonic generation. A single alternating field generates only odd harmonics; absence of even harmonics is a consequence of the scattering cross section symmetry with respect to the inversion of the electron velocity direction and of the isotropy of the initial Maxwellian electron velocity distribution function. Both the addition of a static electric field or the mixing of two oscillating fields, having an integer ratio between the two frequencies, can break the inversion symmetry and generate also even harmonics, resulting, therefore, a sensitive means for the control of the emission rates of both even and odd harmonics. Indeed, it has been shown that an opportune manipulation of the relative intensity and polarization of the two fields, offers the possibility to produce coherent radiation beyond that achievable with a single field (Alekseev et al., 1999; Persano Adorno et al., 2003a;b; Romanov et al., 2004).

In the last decade, in order to better understand the harmonics emission process in atoms, gases and plasmas, in the presence of two laser fields, and to enhance its use in applications, several studies have been focused on the investigation of the harmonic polarization properties (Borca et al., 2000; Dudovich et al., 2006; Ferrante et al., 2000; 2004a;b; 2005; Song et al., 2003; Wang et al., 1999; Xia et al., 2007). In atoms, even for a linearly polarized driving laser, in the presence of an additional constant electric field, the harmonics are in general elliptically polarized (Borca et al., 2000). Moreover, the introduction of a second linearly polarized laser beam at low-intensity, collinear with the first one, can produce unusual polarization features of the generated harmonics (Borca et al., 2000). In plasmas driven by a laser field, in the presence of an additional electric static field, it has been found that the even polarization plane rotates with respect to that of the laser field and that the value of the rotation angle depends on the harmonic number (Ferrante et al., 2004a;b; 2005). This circumstance could allow to use harmonics also as a diagnostic tool (Mairesse et al., 2008).

Although the conversion efficiency in semiconductors subjected to two alternating electric fields has extensively been investigated, to the best of our knowledge, very little has been done in the study of the polarization of the emitted radiation. The primary focus of this part of the chapter is to show the effect of mixing two color fields, having an integer ratio between the two frequencies, on the polarization of both even and odd harmonics, that are generated in a low-doped GaAs bulk. We study the polarization of even and odd harmonics as a function of the angle between the direction of the two applied fields and compare the polarization obtained from the mixing of an oscillating field with a static electric field with that obtained in the presence of two periodic fields (Persano Adorno et al., 2007b; Persano Adorno, 2010).

3.2 Harmonic generation theory

The propagation of an electromagnetic wave along the z direction in a medium is described by the Maxwell equation

$$\frac{\partial^2 \overrightarrow{E}}{\partial z^2} - \frac{1}{c^2}\frac{\partial^2 \overrightarrow{E}}{\partial t^2} = \mu_0 \frac{\partial^2 \overrightarrow{P}}{\partial t^2} \tag{1}$$

where

$$\overrightarrow{P} = \varepsilon_o(\chi_1 + \chi_2 E + \chi_3 E^2 + ...)\overrightarrow{E} \tag{2}$$

is the polarization of the free electron gas in terms of the linear χ_1 and nonlinear $\chi_2, \chi_{3,...}$susceptibilities.
The source of the nonlinearity is the current density

$$\overrightarrow{j} = -ne\overrightarrow{v}(\overrightarrow{E}) \tag{3}$$

related to the polarization $\overrightarrow{P}$ by

$$\overrightarrow{j} = \frac{\partial \overrightarrow{P}}{\partial t} \tag{4}$$

Expanding the electrons velocity and the electric field in terms of their Fourier components as

$$\overrightarrow{v} = \sum_q \overrightarrow{v}_q \exp\{-iq(\omega t - kz)\} \tag{5}$$

$$\overrightarrow{E} = \sum_q \overrightarrow{E}_q \exp\{-iq(\omega t - kz)\} \tag{6}$$

with $\omega = 2\pi\nu$, and taking only the leading term in the nonlinear part of the q-th component of the polarization $\overrightarrow{P}$

$$\overrightarrow{P}_q^{NL} = \varepsilon_o \chi_q \overrightarrow{E}_1^q \tag{7}$$

we obtain a relation between the q-th component of the velocity and the susceptibility χ_q given by

$$\chi_q = -\frac{inev_q}{q\omega E_1^q} \tag{8}$$

If we substitute the expansion for the electric field and use the above relation in the Maxwell equation, we obtain

$$\overrightarrow{E_q}[-q^2k^2 + \frac{1}{c^2}q^2\omega^2] = i\mu_0 q\omega ne\overrightarrow{v_q} \tag{9}$$

By limiting the study of the harmonic generation efficiency to thin samples so as to reduce the loss, it is possible to not consider in the calculations the complex form of the dielectric function $\epsilon(\nu)$ and neglect the field-dependent absorption. Assuming that the medium is transparent to the radiation at frequency ν, i.e. $\nu > \nu_p$, ν_p being the donor plasma frequency, we can use the dispersion relation and calculate the efficiency of the harmonic generation at frequency $\nu = q\nu_1$, normalized to the fundamental one ν_1, as (Persano Adorno et al., 2000; 2001):

$$\frac{I_\nu}{I_{\nu_1}} = \frac{1}{q^2}\frac{v_\nu^2}{v_{\nu_1}^2} \tag{10}$$

where v_ν is the Fourier transform of the electron drift velocity, obtained via the three-dimensional multivalleys Monte Carlo simulation of the electron motion in the semiconductor. The spectra of emitted radiation are then reconstructed by the analysis of the velocity Fourier components.

3.3 Results and discussion

In all simulations the lattice temperature is $T = 80$ K. The results are obtained in a stationary regime, after a transient time of a few picoseconds has elapsed. In all runs it is always present a linearly polarized oscillating electric field $E_1(t)$, having amplitude $E_1 = 30$ kV/cm and frequency $\nu_1 = 200$ GHz, which can rotate in the plane xy; the effects on the harmonic generation process due to the introduction of a second field are studied. In order to investigate the polarization of the emitted radiation, as a function of the different geometries of the linear polarization of the two incident fields, the harmonic spectra along the x- and y-axis have been computed.

3.3.1 Additional static field

We consider the GaAs bulk under the influence of the sum of the $E_1(t)$ field with a constant electric field $E_0 = \beta E_1$, with β constant. The total field is described by the components:

$$E_x(t) = E_1 \cos(\varphi) \cos(2\pi\nu_1 t - k_1 z) + E_0 \tag{11}$$

$$E_y(t) = E_1 \sin(\varphi) \cos(2\pi\nu_1 t - k_1 z) \tag{12}$$

where φ is the angle between the static field E_0, directed along the x-axis, and the oscillating field $E_1(t)$, lying in the plane xy. The additional static electric field, by lowering the symmetry of the system, allows the generation of even harmonics, whose amplitudes increase with the strength of the static field (Persano Adorno et al., 2007b).

To choose the amplitude of the additional static field to be used to analyze the harmonic generation also for different geometries of the linear polarization of the two incident fields, a preliminary analysis of the efficiency of the generated harmonics, as a function of β, has been done.

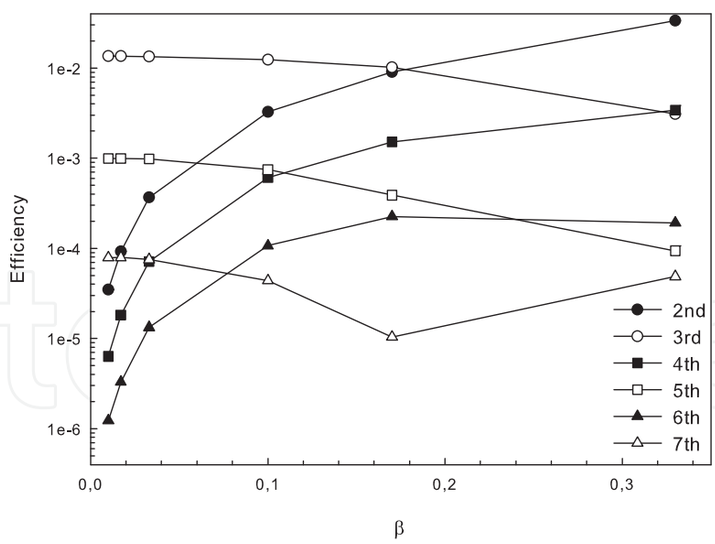

Fig. 1. Efficiency of the first harmonics as a function of $\beta = E_0/E_1$, calculated with $E_1 = 30$ kV/cm and $\nu_1 = 200$ GHz.

In Figure 1 we show the intensity of the first harmonics obtained with the total electric field directed along the x-axis ($\varphi = 0^o$). For $\beta \geqslant 0.1$ even and odd harmonics have comparable intensities; accordingly, to study the polarization of the emitted radiation, we adopt $\beta = 0.1$, i.e. $E_0 = 3$ kV/cm, in all simulations.

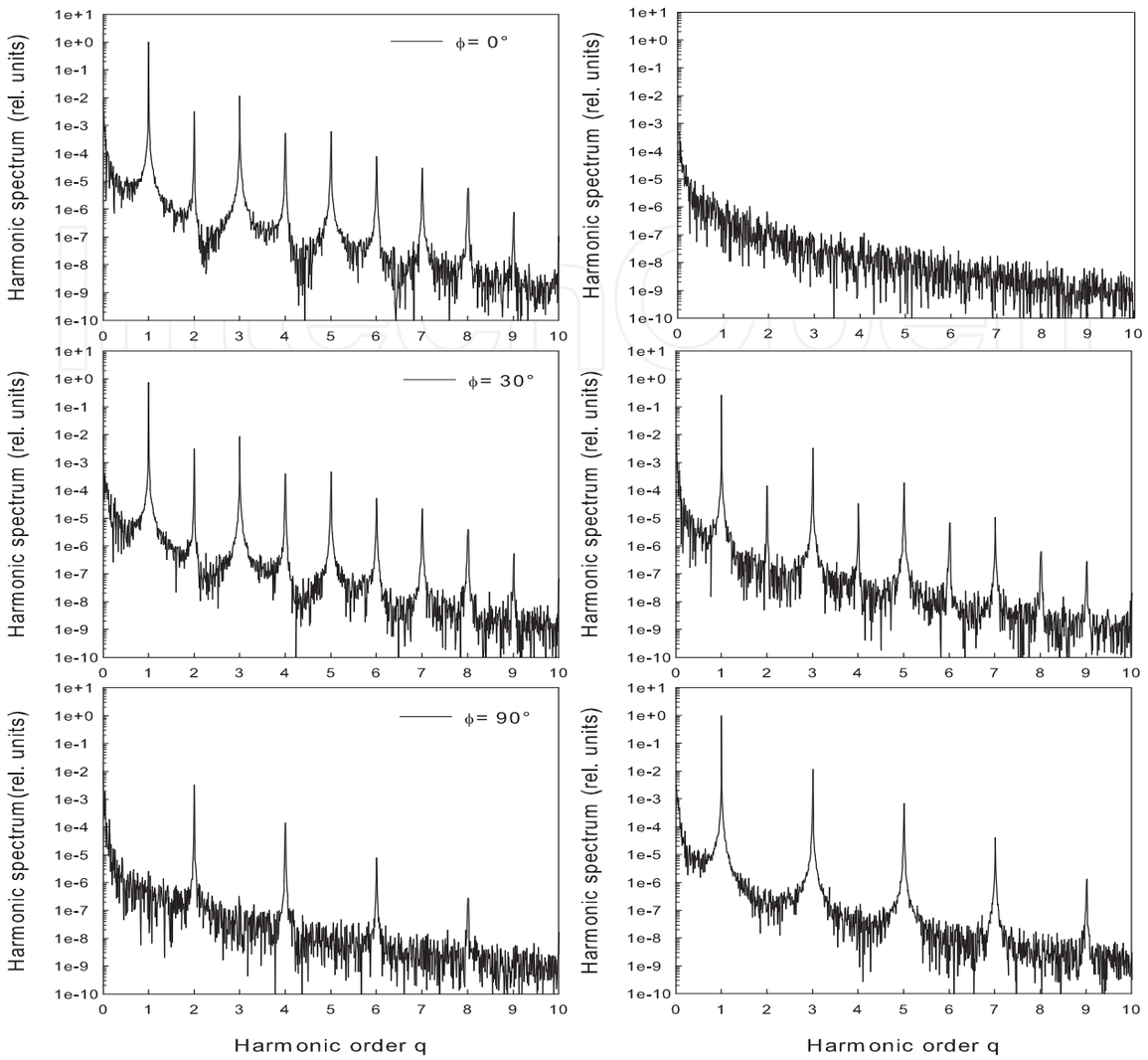

Fig. 2. Harmonic spectra along x-axis (left panels) and y-axis (right panels) at different φ as a function of the harmonic order q. $E_1 = 30$ kV/cm, $\nu_1 = 200$ GHz, $\beta = 0.1$.

Figure 2 shows the harmonic spectra along the x and the y-axis for different values of the angle φ. When $\varphi = 0^o$, along the x-axis we find, as expected, odd and even harmonics, and noise along the y-axis. Less obvious is the behaviour of the harmonic peaks when the two fields are not parallel, since the efficiency of both odd and even harmonics becomes function of the angle φ. In particular, when $\varphi \neq 0^o$, the spectrum along the y-axis contains non negligible even harmonics due to the presence of the static field, although along the y direction is present only $E_1(t)$. When $\varphi = 90^o$ the spectrum along the x-axis shows only the even harmonics of the oscillating field, perpendicular to this direction, while along the y direction the spectrum contains only odd harmonics.

Figure 3 shows the angle α between the x-axis and the direction of the first four even (upper panel) and odd harmonics (lower panel), as a function of the angle φ. Since the static field strength is small compared to the amplitude of E_1, odd harmonics are nearly polarized in the same direction of the sub-THz field. On the contrary, the coincidence of the polarization angle

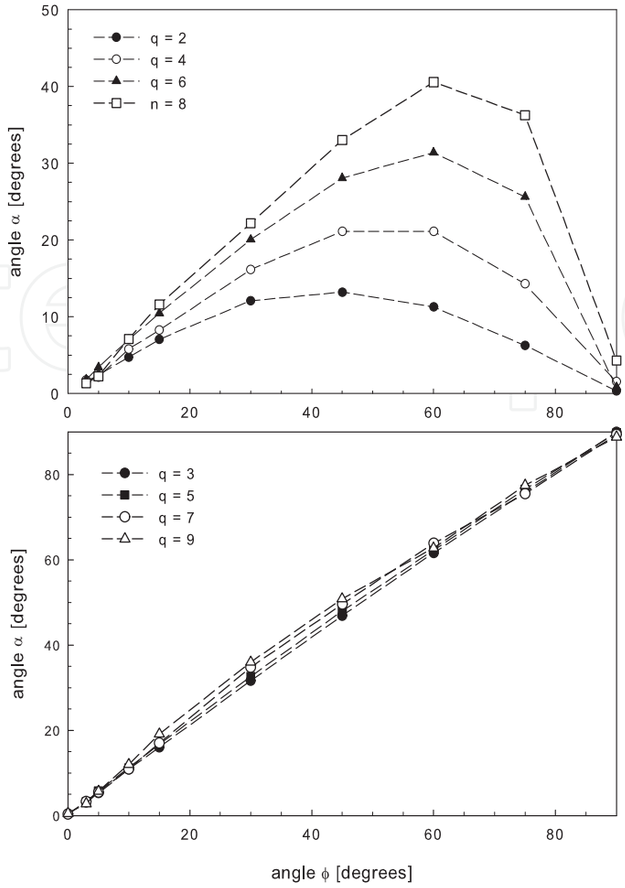

Fig. 3. Polarization angle α of even (upper panel) and odd (lower panel) harmonics generated by the GaAs bulk as a function of the angle φ. $E_1 = 30$ kV/cm, $\nu_1 = 200$ GHz, $\beta = 0.1$.

with that of the static field is not found for even harmonics. Moreover, even harmonics show a different polarization angle for each harmonic order. This behavior is close to that noted in a theoretical study of laser even harmonic generation by a plasma embedded in a static electric field (Ferrante et al., 2004a;b; 2005). Initially, for $\varphi < 20^o$, even harmonics are polarized nearly in the same direction of E_1, then for $20^o < \varphi < 60^o$, the angle α increases more slowly than φ and this effect appears more evident for lower values of the harmonic number q. Finally, for $\varphi > 60^o$ the polarization angle strongly decreases and, when $\varphi = 90^o$, even harmonics are directed along the x-axis, as the constant field.

3.3.2 Additional oscillating field

The asymmetry effect induced by the presence of a static field may be also introduced by a second periodic field. In order to explore this case, we consider the GaAs bulk under the influence of a linearly polarized periodic electric field $E(t)$ given by the sum of $E_1(t)$ with a low-intensity field $E_2(t)$, having amplitude $E_2 = 3$ kV/cm and frequency ν_2= 0.5 ν_1, described by the components:

$$E_x(t) = E_1 \cos(\varphi) \cos(2\pi\nu_1 t - k_1 z) + E_2 \cos(2\pi\nu_2 t - k_2 z) \quad (13)$$

$$E_y(t) = E_1 \sin(\varphi) \cos(2\pi\nu_1 t - k_1 z) \quad (14)$$

where φ is the angle between the field $E_2(t)$, directed along the x-axis, and the field $E_1(t)$, lying in the plane xy.

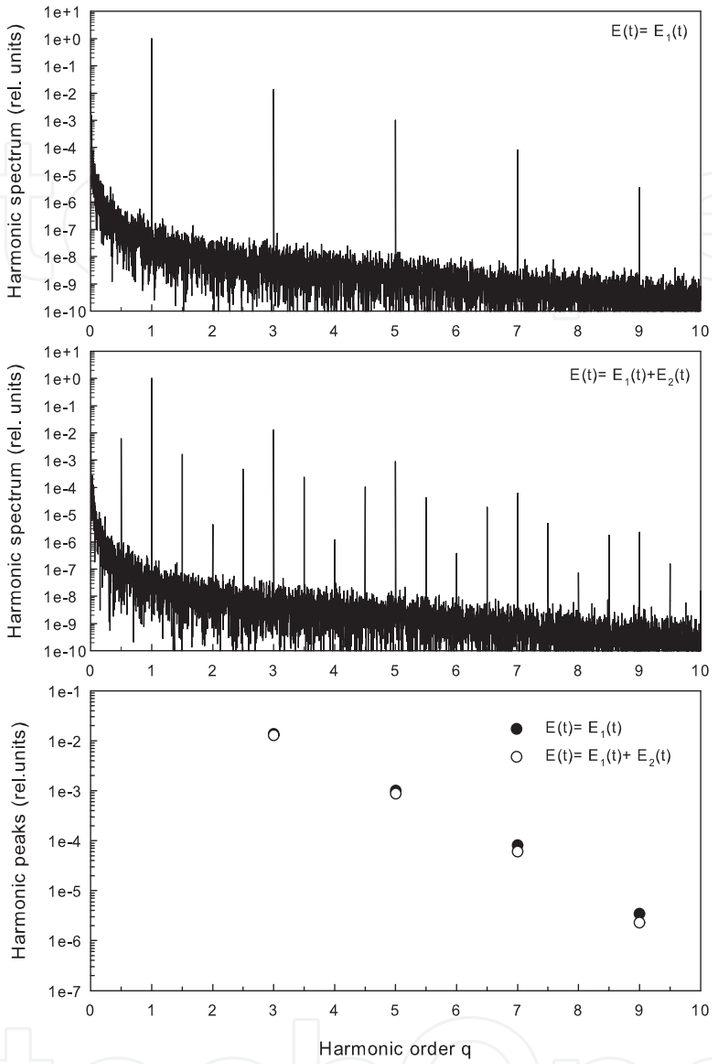

Fig. 4. Harmonic spectra obtained with the E_1 field only (upper panel) and the E_2 field parallel to the E_1 field (central panel) as a function of the harmonic order q. Bottom panel show the intensity of the odd harmonic peaks in the two cases. $E_1 = 30$ kV/cm, ν_1=200 GHz, $E_2 = 3$ kV/cm, ν_2=100 GHz; $\varphi = 0^o$.

Harmonic spectra obtained with the $E_1(t)$ field only (upper panel) and the $E_2(t)$ field parallel to the $E_1(t)$ field (central panel) are shown in Figure 4. When the two fields are parallel we found an enrichment of the spectrum with respect to the expected generation of odd harmonics of each field, because of the presence of satellite harmonics at mixed frequencies. In particular, as shown in the bottom panel of Figure 4, under field mixing conditions the peaks at the odd harmonics of the strong driving field frequency are present with amplitude nearly unchanged. Additionally, thanks to the nonlinear sum-frequency process, between pairs of odd harmonics of the frequency ν_1, there are three peaks due to the presence of the field $E_2(t)$. This spectrum is very similar to that found in an experimental work on the generation of

harmonics in atomic gases (Perry & Krane, 1993). The intensity of these three additional peaks strongly depends on the relative angle between the two oscillating fields (see Figure 5).

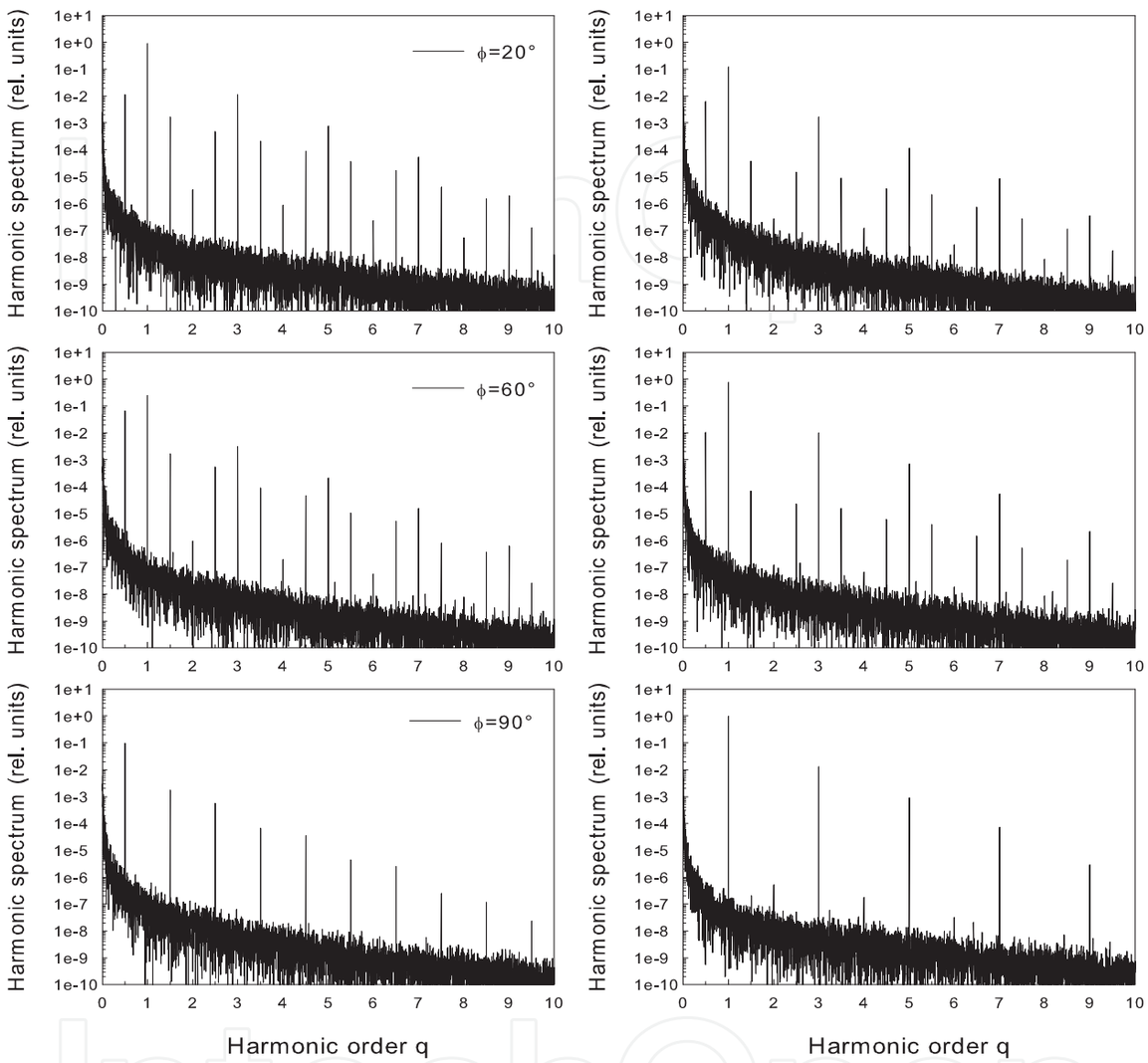

Fig. 5. Harmonic spectra along x-axis (left panels) and y-axis (right panels) at different φ as a function of the harmonic order q. $E_1 = 30$ kV/cm, ν_1=200 GHz, $E_2 = 3$ kV/cm, ν_2=100 GHz.

When the field $E_1(t)$ has a component different from zero along the y-axis, also the spectrum along this axis contains the three additional peaks due to the presence of the $E_2(t)$ field, although along the y direction is present only the field $E_1(t)$. When the fields are orthogonal, i.e. $\varphi = 90^o$, the spectrum along the y-axis still contains the even harmonics, while the peaks immediately on either side of the odd harmonics of the frequency ν_1 disappear; the spectrum along the x-axis contains only harmonics corresponding to odd multiples of the frequency ν_2. As discussed in Ref. (Perry & Krane, 1993), the peak between the odd harmonics of the frequency ν_1, which corresponds to an even harmonic of ν_1, can be justified as true "even" harmonic, resulting from symmetry breaking of the Hamiltonian due to the presence of $E_2(t)$, or as resulting from different combinations of the two frequencies, as, for instance, from the sum of an odd harmonic of ν_1 plus the second harmonic of ν_2. Also the peaks immediately on

each side of the odd harmonics of the frequency ν_1 can be attributed to true "odd" harmonics of $E_2(t)$ or, for example, to the combination of an even harmonic of ν_1 plus or minus the signal at ν_2. The analysis of the polarization of the emitted harmonics can help to highlight this aspect. Actually, the polarization of true "even" harmonics in two-colors experiment would be qualitatively similar to that predicted for an alternating field plus a static field, as long as the ratio of field strengths is comparable. Figure 6 shows the harmonic polarization plane for harmonic radiation corresponding to even (upper panel) and odd (central panel) multiples of the frequency ν_1, as a function of the angle φ between the two oscillating fields. In the bottom panel is instead plotted the polarization angle of harmonics corresponding to odd multiples of the frequency ν_2. Also in this case, "even" harmonics show different polarization plane for different harmonic order. Nevertheless, the dependence of the polarization angle α on the relative direction of the two fields is different with respect to the case in which the even harmonics are due the introduction of a static electric field. In particular, in the presence of two periodic fields, for $\varphi < 20^o$, "even" order harmonics are polarized nearly in the same direction of the strong field $E_1(t)$ and for $20^o < \varphi < 60^o$ the angle α increases more slowly than φ. Rather, for lower values of the harmonic number q, α remains almost constant. Instead, for $\varphi > 60^o$ the polarization angle strongly increases and at $\varphi = 90^o$, "even" harmonics are directed along the y-axis. On the other hand, also the polarization plane of the "odd" harmonics of the frequency ν_2 does not coincide with the direction of the field $E_2(t)$, but it shows a dependence on the angle φ. Unexpectedly, the first "odd" harmonic is polarized up to $\sim 40^o$ from the direction of $E_2(t)$. The polarization angle of the other three "odd" harmonics appears to be only slightly dependent on the angle φ, keeping it nearly constant at $\sim 15^o$, from the direction of $E_2(t)$.

3.4 Conclusions

By mixing a strong field with a weak field, oscillating at a frequency whose value is half of that of the high-intensity one, it is possible produce sum and difference-frequency radiation, including odd and even harmonics. The field-mixing does not affect the efficiency of the odd harmonics of the strong field and makes the spectra more rich. The behavior shown by the "even" harmonics shares some features with those occurring in the presence of an additional constant electric field, as, for example, the circumstance that even harmonics show different polarization plane for different harmonics order. However the dependence of the polarization angle of these "even" harmonics on the angle between the two incident fields, does not coincide with that obtained in the presence of an additional static electric field. On the contrary, for the odd harmonics of the high-intensity field there is no rotation of the polarization plane. Moreover, because the polarization angle of the "odd" harmonics of the low-frequency field does not coincide with its direction, we can conclude that these are not true "odd", but, as the "even" ones, are mainly due to the sum-frequency process.

4. Noise enhanced stability in semiconductor systems

4.1 A brief introduction to the problem

The presence of noise in experiments is generally considered a disturbance, especially studying the performance of semiconductor-based devices, where strong fluctuations can affect their response. Recently, however, an increasing interest has been directed towards the constructive aspects of noise on the dynamical response of non-linear systems. The effect of the interaction between an external source of fluctuations and an intrinsically noisy system has been analytically investigated for the first time by Vilar and Rubí in 2001. They have

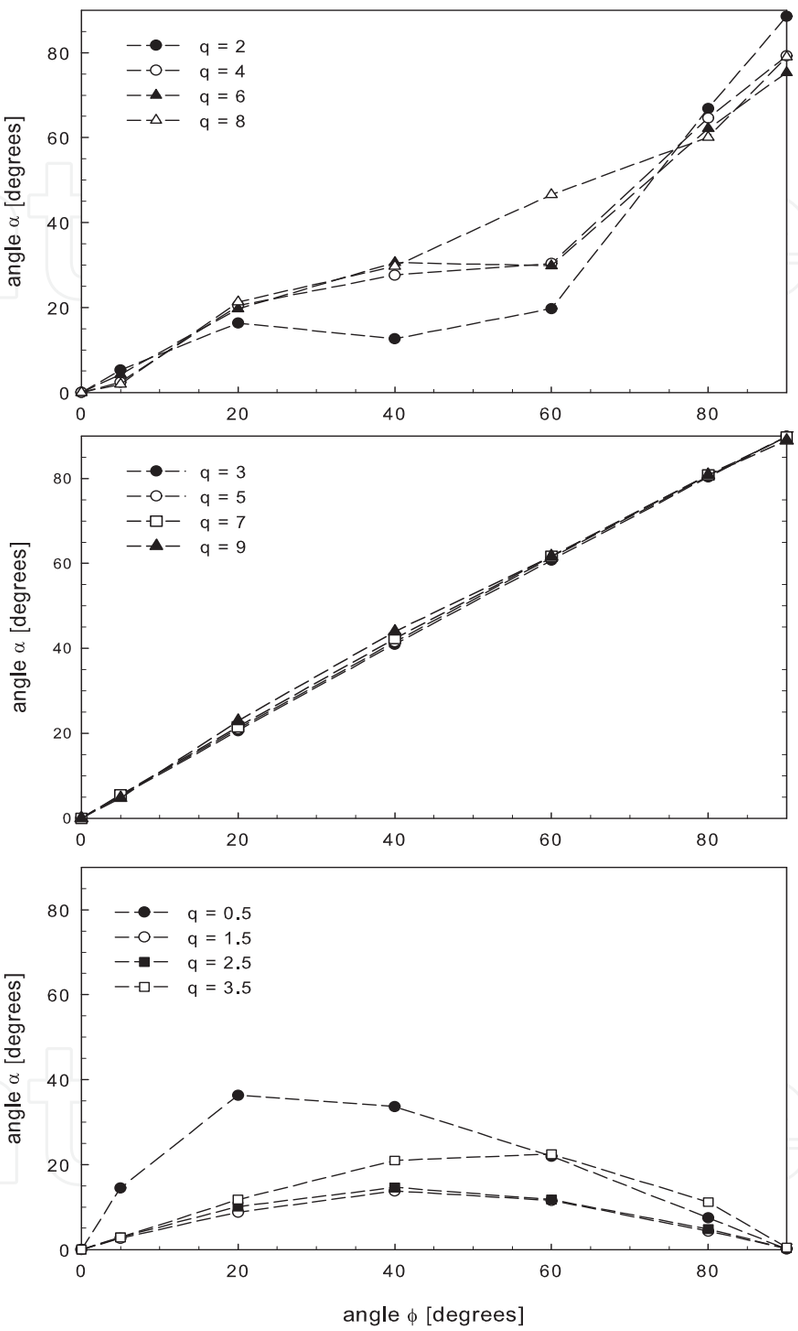

Fig. 6. Polarization angle α of the generated harmonics as a function of the angle φ. Upper and central panels show "even" and odd harmonics of the frequency ν_1,respectively; the bottom panel refers to "odd" harmonics of the frequency ν_2. $E_1 = 30$ kV/cm, ν_1=200 GHz, $E_2 = 3$ kV/cm, ν_2=100 GHz.

demonstrated that the spectral intensity of the output signal in a low frequency domain can be reduced by the addition of small amplitude noise on the input of the system (Vilar & Rubí, 2001).

In semiconductor bulk materials the possibility to reduce the diffusion noise by adding a correlated random contribution to a driving static electric field has been investigated by Varani and collaborators. Their numerical results, obtained by including energetic considerations in the theoretical analysis, have shown that, under specific conditions of the fluctuating electric field, it is possible to suppress the intrinsic noise in n-type GaAs semiconductors (Varani et al., 2005).

Recent studies of the electron velocity fluctuations in GaAs bulks driven by periodic electric fields, have shown that the spectral density strongly depends on the frequency of the applied field and critical modifications are observed when two mixed high-frequency large-amplitude periodic electric fields are used (Persano Adorno et al., 2008a). This means that the total power spectrum of the intrinsic noise is dependent on both the amplitude and the frequency of the excitation signals.

In this part of the chapter we focus our attention on the noise influence on the intrinsic carrier noise spectral density in low-doped n-type GaAs semiconductor driven by a high-frequency periodic electric field (Persano Adorno et al., 2008b; 2009a). The semiconductor intrinsic noise is obtained both by computing the velocity fluctuations correlation function and the spectral density (González et al., 2003; Shiktorov et al., 2003b) and directly calculating the variance of the electron velocity fluctuations. The effects caused by the addition of an external source of random perturbations are investigated by analyzing (i) the noise spectral density at the same frequency of the external driving field and (ii) the integrated spectral density (ISD), for different values of both the external noise amplitude and the noise correlation time. Numerical results show that, strictly depending on the correlation time, the presence of the external noise modifies the electron average velocity and significantly affects both the correlation function of its fluctuations and the internal noise spectrum of the system.

4.2 Semiconductor noise calculation

The semiconductor bulk is driven by a fluctuating periodic electric field

$$E(t) = E_1 \cos(\omega t + \phi) + \eta(t) \tag{15}$$

with frequency $\nu = \omega/2\pi$ and amplitude E_1. The random component of the electric field is modeled with an Ornstein-Uhlenbeck (OU) stochastic process $\eta(t)$, which obeys the following stochastic differential equation:

$$\frac{d\eta(t)}{dt} = -\frac{\eta(t)}{\tau_c} + \sqrt{\frac{2D}{\tau_c}}\xi(t) \tag{16}$$

where τ_c and D are, respectively, the correlation time and the variance of the OU process, and $\xi(t)$ is the Gaussian white noise with the autocorrelation $< \xi(t)\xi(t') >= \delta(t - t')$. The OU correlation function is $< \eta(t)\eta(t') >= D \exp(-|t - t'|/\tau_c)$. The changes on intrinsic noise properties are investigated by the statistical analysis of the autocorrelation function of the velocity fluctuations and of its mean spectral density. When the system is driven by a periodic electric field the correlation function $C_{\delta v \delta v}(t, \tau)$ of the velocity fluctuations $\delta v(t) = v(t) - \langle v(t) \rangle$ can be calculated as (González et al., 2003)

$$C_{\delta v \delta v}(t, \tau) = \left\langle v\left(t - \frac{\tau}{2}\right) v\left(t + \frac{\tau}{2}\right) \right\rangle - \left\langle v\left(t - \frac{\tau}{2}\right) \right\rangle \left\langle v\left(t + \frac{\tau}{2}\right) \right\rangle \tag{17}$$

in which τ is the correlation time and the average is meant over a sequence of equivalent time moments $t = s + mT$, with s belonging to the time interval $[0, T]$ (T is the field period) and m is an integer. This two-time symmetric correlation function eliminates any regular contribution and describes only the fluctuating part of $v(t)$. By averaging over the whole set of values of t within the period T, the velocity autocorrelation function becomes

$$C_{\delta v \delta v}(\tau) = \frac{1}{T} \int_0^T C_{\delta v \delta v}(t, \tau) dt \tag{18}$$

As due to the Wiener-Kintchine theorem, the spectral density can be calculated as the Fourier transform of $C_{\delta v \delta v}(\tau)$. In the computations of the autocorrelation function we have considered 10^3 possible initial values of s and a total number of equivalent time moments $m \cong 10^6$.
Intrinsic noise has been investigated also by estimating directly the electron velocity variance. This calculation has been performed separately for each energy valley, following the same method of equivalent time moments described above (Persano Adorno et al., 2009a).

4.3 Physical model of intrinsic noise

When the semiconductor is driven by a static electric field, the shape of the spectral density of electron velocity fluctuations is exclusively determined by the strength of the applied field. For amplitudes smaller than the threshold field E_G (Gunn Field) for intervalley transitions, the diffusion is the most relevant source of noise, while, for $E_0 > E_G$, the complex structure of the semiconductor becomes relevant and random transitions of carriers among the available energy valleys must be taken into account. In this case, the intrinsic noise is mainly determined by a partition noise, caused by stochastic carrier transitions between regions characterized by different dynamical properties (intervalley transfers) in momentum space. The partition noise is characterized by a pronounced peak in the spectral density at a frequency ν_G, which can be defined the "natural" transition frequency of the system between the valleys (Persano Adorno et al., 2008a).
Under cyclostationary conditions, the noise behaviour depends on both the amplitude and the frequency of the applied field. In particular, it is similar to that of the static field case only for very low-frequency fields ($\nu \ll \nu_G$). On the contrary, for frequencies $\nu \gtrsim \nu_G$, the intervalley transfers are driven by the external field, the system enters in a forced regime of oscillations and the velocity fluctuations become time correlated (Persano Adorno et al., 2008a). In this case, the spectral density exhibits a peak centered around the frequency of the periodic signal and a significant enhancement in the low-frequency region.

4.4 Numerical results and discussion

In order to neglect thermal noise contribution and to highlight the partition noise effects we have chosen as lattice temperature $T = 80$ K. The spectral density of the electron velocity fluctuations has been studied by adopting a fluctuating periodic electric field with frequency $\nu = 500$ GHz. The amplitude of this field has been chosen on the base of a preliminary analysis of both the variance of velocity fluctuations and the spectral density $S_0(E)$ at zero frequency, as a function of the amplitude of the oscillating field. The most favorable condition to obtain a noise suppression effect in our system is reached when $d^2 S_0(E)/dE^2$ is negative and the variance of velocity fluctuations exhibits a maximum (Varani et al., 2005; Vilar & Rubí, 2001). In accordance with the results shown in figures 1a and 1b of Ref. (Persano Adorno et al., 2009a), we have chosen a driving electric field with amplitude $E_1 = 10$ kV/cm and frequency $\nu = 500$ GHz.

In the absence of external noise, the amplitude of the forcing field is large enough to switch on intervalley transitions from the Γ valley to the L valleys and, since the frequency ν is of the same order than ν_G, the electron velocity fluctuations are mainly determined by partition noise (Shiktorov et al., 2003b). Hence, the spectrum is characterized by the features described in section 4.3

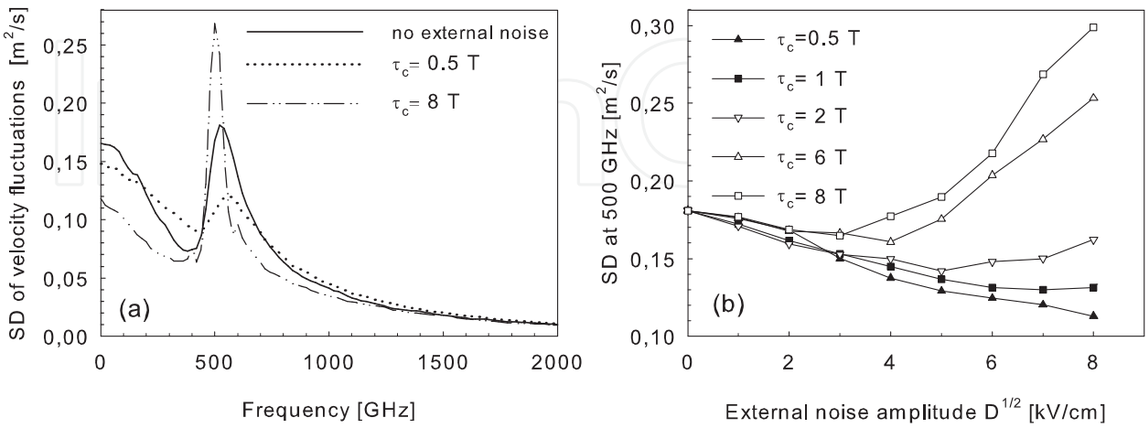

Fig. 7. (a) Spectral density (SD) of electron velocity fluctuations as a function of the frequency. Solid line is obtained in the absence of external noise; dotted line describes the results obtained with $D^{1/2} = 7$ kV/cm and $\tau_c = 1$ ps $= 0.5\ T$; dashed-dotted line is obtained with $D^{1/2} = 7$ kV/cm and $\tau_c = 16$ ps $= 8\ T$. (b) Height of the peak in the SD of electron velocity fluctuations as a function of the external noise amplitude for different values of the correlation time τ_c of the external noise source.

In figure 7a we show how the spectral density of electron velocity fluctuations is modified by the presence of noise. The addition of an external source of fluctuations to the driving electric field strongly changes the spectrum and, in particular, the height of the peak around 500 GHz, in a way that critically depends on the OU correlation time. In figure 7b we plot the maximum of the spectral density at the frequency of the driving field as a function of the external noise amplitude $D^{1/2}$, for five different values of τ_c. An interesting nonlinear behavior of this quantity is observed for increasing noise intensities and correlation times. In particular, for values of τ_c smaller than or equal to the period T of the oscillating electric field, the spectral density at 500 GHz shows a monotonic decreasing trend with increasing noise amplitude. For values of τ_c greater than T, the spectral density is reduced only for small amplitudes of the external noise, while an enhancement of the peak is observed for greater intensities. When the intrinsic noise is mainly due to the partition effect, the height of the peak in the spectral density depends on the population of the different valleys and it reaches a maximum when the populations are nearly at the same level (Nougier, 1994; Shiktorov et al., 2003b). Since the "effective" electric field experienced by electrons in the presence of a fluctuating field is different, the number of intervalley transitions changes with respect to the case in which the external source of noise is absent. This fact can be responsible of the observed changes on the peak of the spectral density.

The dependence of the intrinsic noise suppression effect on the amplitude and the correlation time of the external source of fluctuations has been investigated also by studying the integrated spectral density (ISD), i. e. the total noise power, as a function of the OU noise amplitude, for three different values of τ_c. In figure 8 we show a clear reduction of the ISD in the presence of added noise. In particular, for each value of the correlation time, we find a

range of $D^{1/2}$ in which the electric field fluctuations reduce the semiconductor intrinsic noise. This effect is more evident for higher correlation times.

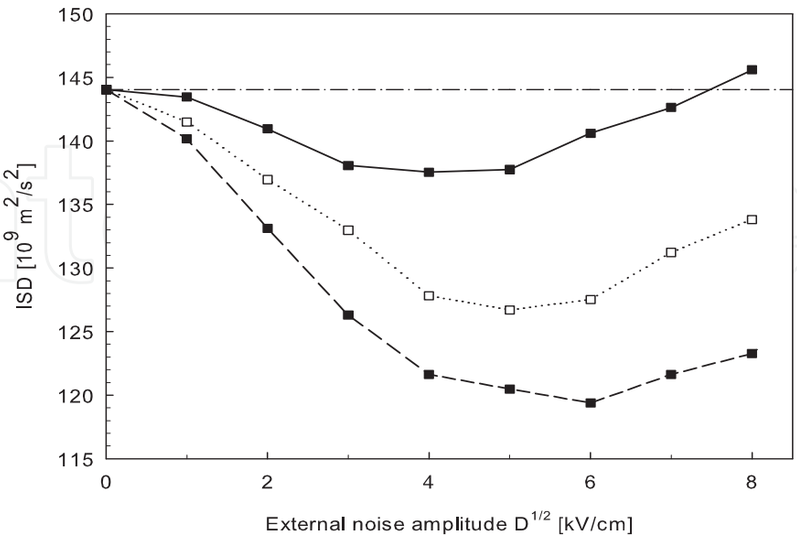

Fig. 8. Integrated spectral density of electron velocity fluctuations as a function of the external noise amplitude. Solid line: $\tau_c = 0.5\ T$; dotted line: $\tau_c = 2\ T$; dashed line: $\tau_c = 8\ T$. Dashed-dotted line is the semiconductor intrinsic noise level

From a microscopic point of view, this suppression can arise from the fact that the fluctuating electric field forces the carriers to visit regions of the momentum space characterized by a smaller variance with respect to the case of zero noise (Walton & Visscher, 2004). We have investigated the details of the electron dynamics under the fluctuating electric field by analyzing for different correlation times the relative occupation time and the velocity variance separately in different valleys. In figure 9 (right panels) we show that, when the noise amplitude increases, the electron occupation time of the Γ valley decreases and the corresponding times calculated for the L and X valleys increase. This behavior is expected because the addition of fluctuations to the driving electric field leads to an increase of scattering events which are responsible for an increase of the transitions from the Γ valley to valleys at higher energy. This behavior depends on the correlation time of the external noise source. In particular, for a fixed value of the external noise intensity, the effect of reduction of the relative occupation time for the Γ valley and the corresponding increase for the L valleys is more pronounced for shorter correlation times.

Less obvious is the behavior of the electron velocity variance evidenced in figure 9 (left panels). In fact, while the common experience would suggest an increase of the velocity variance when the external noise amplitude grows up, we find that, depending on the value of the correlation time, the velocity variance in the Γ valley can be reduced in a specific range of the noise amplitude. An increasing trend is instead observed for the L and X valleys. The reduction of the electron velocity variance observed in the Γ valley for $\tau_c = 2\ T$ and $D^{1/2}$ between 1 and 6 and, even more, for $\tau_c = 8\ T$ and $D^{1/2}$ between 1 and 8, represents an intrinsic effect of the dynamics of electrons in the Γ valley without taking into consideration any transfer to valleys characterized by different dynamical properties. This effect of noise-induced stability can explain the longer residence times of electrons in the Γ-valley at higher correlation times.

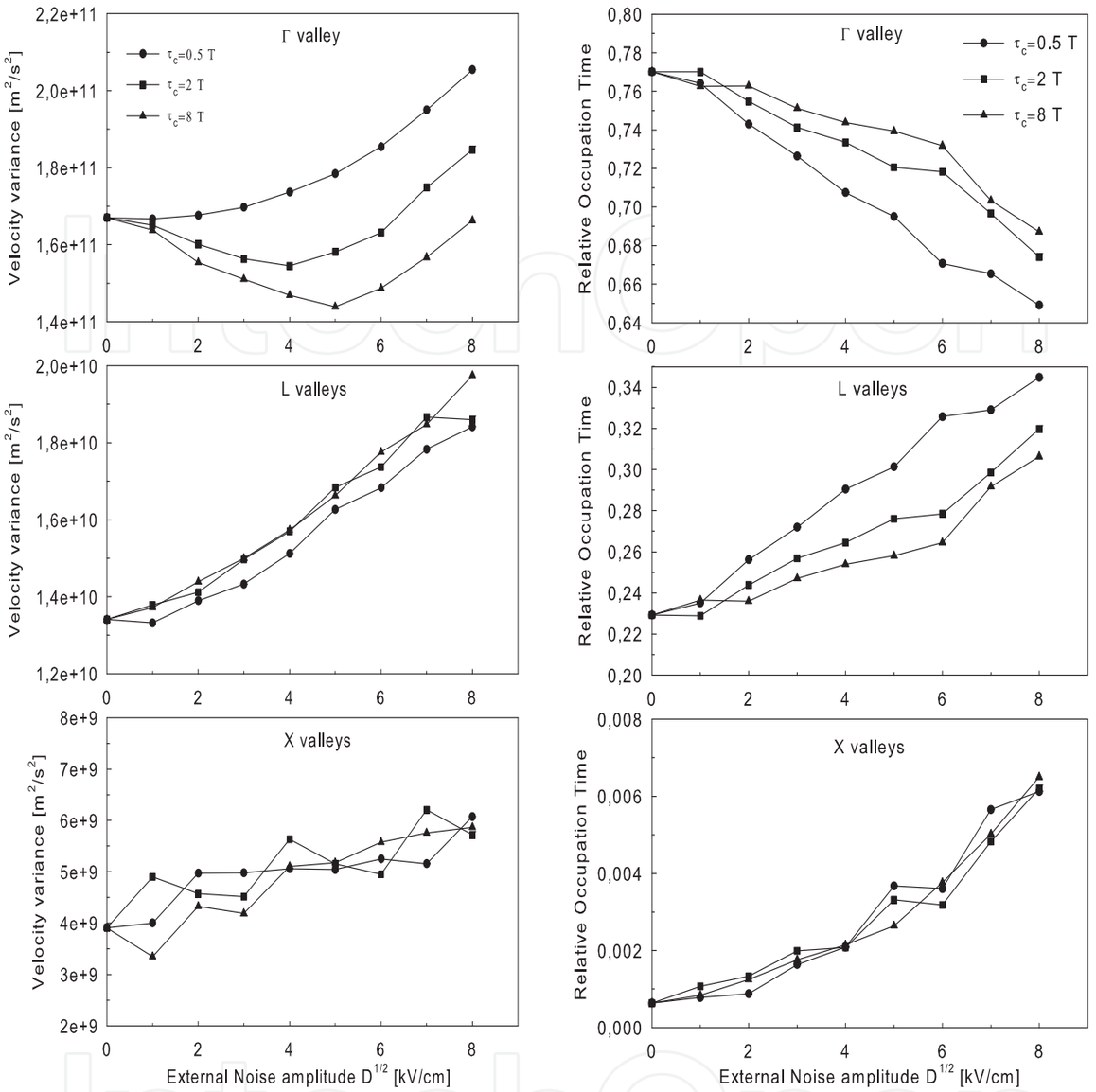

Fig. 9. Variance of the electron velocity fluctuations (left panels) and relative occupation time (right panels) as a function of the external noise amplitude, for three different correlation times.

4.5 Conclusions

A less noisy response in the presence of a driving periodic electric field containing time-correlated fluctuations is observed. Both the amplitude and the correlation time of the electric field fluctuations are crucial parameters for the intrinsic noise reduction effect. Previous studies ascribe the reduction of the electron velocity fluctuations to an overall effect of intervalley transfers. Our study on the electron velocity variance, calculated separately for every single energy valley of the semiconductor, shows that the velocity variance of an electron moving in the Γ-valley is reduced by the presence of correlated noise, independently from the transitions to upper valleys, bringing to longer residence times. This effect of noise enhanced stability (NES) arises from the fact that the transport dynamics of electrons in the

semiconductor receives a benefit by the constructive interplay between the fluctuating electric field and the intrinsic noise of the system.
Moreover, for a fixed value of the external noise amplitude, a very unexpected non-monotonic behavior of the integrated spectral density as a function of the noise correlation time, in a wider range of τ_c, is discussed in (Persano Adorno et al., 2009b).

5. Influence of transport conditions on the electron spin depolarization

5.1 Preliminary remarks

For an extensive utilization of spintronic devices, the features of spin decoherence at relatively high temperature, jointly with the influence of transport conditions, should be fully understood. In last decade there has been a lot of experimental works in which the influence of transport conditions on relaxation of spins in semiconductors has been investigated (Beck et al., 2006; Dzhioev et al., 2004; Furis et al., 2006; Hägele et al., 1998; Hruška et al., 2006; Kikkawa & Awschalom, 1998; Sanada et al., 2002). Even though for high speed transfer of information, high external electric fields must be used, up now only the influence of low electric fields ($F < 0.1$ kV/cm) on coherent spin transport has been investigated and very little is known about the effects of higher electric fields (Sanada et al., 2002) or high lattice temperatures. Very recently, electrical injection of spin polarization in n-type and p-type silicon at room-temperature have been experimentally carried out (Dash et al., 2009). These promising experimental results for development of spintronic devices suggest that it is important investigate the spin coherence up to room temperature.
The temporal evolution of the spin and the evolution of the momentum of an electron cannot be separated. The spin depolarization rates are functionals of the electron distribution function in momentum space which continuously evolves with time when an electric field is applied to drive the transport. Thus, the dephasing rate is a dynamic variable that needs to be treated self-consistently in step with the dynamic evolution of the electron's momentum. A way to solve this problem is to describe the transport of spin polarization by making use of Boltzmann-like kinetic equations. This can be done within the density matrix approach (Ivchenko et al., 1990), methods of nonequilibrium Green's functions, as the microscopic kinetic spin Bloch equation approach (Jiang & Wu, 2009; Weng & Wu, 2003; Weng et al., 2004; Wu & Ning, 2000; Wu et al., 2010; Zhang et al., 2008), or Wigner functions (Mishchenko & Halperin, 2003; Saikin, 2004), where spin property is accounted for starting from quantum mechanics equations. Another way is to use a Monte Carlo approach, by taking into account the spin polarization dynamics with the inclusion in the code of the precession mechanism of the spin polarization vector (Barry et al., 2003; Bournel et al., 2000; Kiselev & Kim, 2000; Pershin, 2005; Pramanik et al., 2003; Saikin et al., 2003; 2006; Shen et al., 2004; Spezia et al., 2010; Spezia et al., , in press). Both methods allow to include the relevant spin relaxation phenomena for electron systems and take into account the details of electron scattering mechanisms, material properties and specific device design; their predictions have been found to be in good agreement with experiments.
Earlier Monte Carlo simulation has revealed that the presence of an external electric field can accentuate spin relaxation in GaAs bulk materials (Barry et al., 2003). However, a comprehensive theoretical investigation of the influence of transport conditions on the spin depolarization in semiconductor bulk structures, in a wide range of values of temperature, doping density and amplitude of external fields, is still lacking. In this last part of the chapter, solving the transport and spin dynamics stochastic differential equations by a semiclassical Monte Carlo approach, the spin lifetimes and depolarization lengths of an

ensemble of electrons, for intermediate values of the electric field ($0.1 - 2.5$ kV/cm) and lattice temperatures in the range $10 < T < 300$ K, are estimated (Spezia et al., 2010). A detailed analysis of the doping density effect on the fast process of spin depolarization of drifting electrons in GaAs bulks, below the metal-to-insulator transition, can be found in Spezia et al., (in press).

5.2 Spin relaxation dynamics

Spin dephasing may be caused by interactions with local magnetic fields originating from nuclei and spin-orbit interactions or magnetic impurities. The most relevant spin relaxation mechanisms for an electron system under non degenerate regime are: (i) the Elliott-Yafet (EY) mechanism, in which electron spins have a small chance to flip during each scattering, due to the spin mixing in the conduction band (Elliott, 1954; Yafet, 1963); (ii) the Dyakonov-Perel (DP) mechanism, based on the spin-orbit splitting of the conduction band in non-centrosymmetric semiconductors, in which the electron spins decay due to their precession around the **k**-dependent spin-orbit fields (inhomogeneous broadening) during the free flight between two successive scattering events (Dyakonov & Perel, 1971; Dyakonov, 2006); (iii) the Bir-Aronov-Pikus (BAP) mechanism, in which electrons exchange their spins with holes (Bir et al., 1976). Hyperfine interaction is another mechanism, usually important for spin relaxation of localized electrons, but ineffective in metallic regime where most of the carriers are in extended states (Abragam, 1961; Paget et al., 1977; Pikus & Titkov, 1989).
Previous theoretical (Jiang & Wu, 2009; Wu et al., 2010) and experimental (Litvinenko et al., 2010) investigations indicate that the the EY mechanism is totally irrelevant on electron spin relaxation in n-type III-V semiconductors. For this reason we analyze the spin depolarization of drifting electrons in n-type GaAs semiconductors by considering only the D'yakonov-Perel process.
By following the semiclassical formalism, the term of the single-electron Hamiltonian which accounts for the spin-orbit interaction can be written as

$$H_{SO} = \frac{\hbar}{2}\vec{\sigma}\cdot\vec{\Omega}. \tag{19}$$

It represents the energy of electron spins precessing around an effective magnetic field $[\vec{B} = \hbar\vec{\Omega}/\mu_B g]$ with angular frequency $\vec{\Omega}$, which depends on the orientation of the electron momentum vector with respect to the crystal axes. Near the bottom of the Γ-valley, the precession vector can be written as (Pikus & Titkov, 1989)

$$\vec{\Omega}_\Gamma = \beta_\Gamma[k_x(k_y^2 - k_z^2)\hat{x} + k_y(k_z^2 - k_x^2)\hat{y} + k_z(k_x^2 - k_y^2)\hat{z}] \tag{20}$$

In equation (20), k_i ($i = x, y, z$) are the components of the electron wave vector. β_Γ is the spin-orbit coupling coefficient, a crucial parameter for the simulation of spin polarization. In Γ-valley we consider the effects of nonparabolicity on the spin-orbit splitting by using (Pikus & Titkov, 1989),

$$\beta_\Gamma = \frac{\alpha\hbar^2}{m\sqrt{2mE_g}}\left(1 - \frac{E(\vec{k})}{E_g}\frac{9 - 7\eta + 2\eta^2}{3 - \eta}\right) \tag{21}$$

where $\alpha = 0.029$ is a dimensionless material-specific parameter, $\eta = \Delta/(E_g + \Delta)$, with $\Delta = 0.341$ eV the spin-orbit splitting of the valence band, E_g is the energy separation between the conduction band and valence band at the Γ point, m the effective mass and $E(\vec{k})$ the electron energy.

The quantum-mechanical description of electron spin evolution is equivalent to that of the classical momentum $\vec{S}$ experiencing the effective magnetic field, as described by the equation of motion

$$\frac{d\vec{S}}{dt} = \vec{\Omega} \times \vec{S}. \tag{22}$$

Every scattering event changes the orientation of the effective magnetic field $\vec{B}$ (that strongly depends on $\vec{k}$) and the direction of the spin precession axis.

5.3 Calculation of spin depolarization times and lengths

All simulations are performed by using a temporal step of 10 fs and an ensemble of $5 \cdot 10^4$ electrons to collect spin statistics. The initial non-equilibrium spin polarization decays with time as the electrons, driven by a static electric field, move through the medium, experiencing elastic and anelastic collisions. Since scattering events randomize the direction of $\vec{\Omega}$, during the motion, the polarization vector of the electron spin experiences a slow angular diffusion. The dephasing of each individual electron spin produces a distribution of spin states that results in an effective depolarization, which is calculated by ensemble-averaging over the spin of all the electrons.

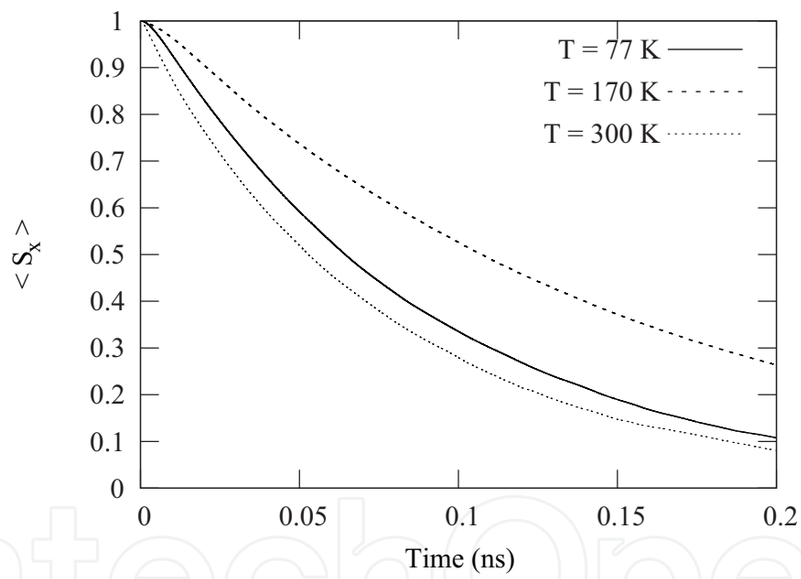

Fig. 10. Spin polarization $\langle S_x \rangle$ as a function of time for three different values of the lattice temperature T, $E_0 = 0.1$ kV/cm.

The simulation of the spin relaxation starts with all the electrons of the ensemble initially polarized ($\langle \vec{S} \rangle = 1$) along the x-axis at the injection plane ($x_0 = 0$). After a transient time of typically 10^4 time steps, long enough to achieve the steady-state transport regime, the electron spins are initialized, the spin relaxation begins and the quantity $\langle \vec{S} \rangle$ is calculated as a function of time. In Fig. 10, we show the electron average polarization $\langle S_x \rangle$, calculated as a function of time in the presence of an electric field, having amplitude $E_0 = 0.1$ kV/cm, directed along the x-axis, for three different values of temperature. In order to extract the characteristic time τ of the spin relaxation, the obtained trend of the spin dephasing is fitted by the following

exponentially time decaying law

$$\langle S_x \rangle(t) = A \cdot exp(-t/\tau), \tag{23}$$

with A a normalization factor. The depolarization length L is the corresponding value of the distance traveled by the center of mass of the electron cloud from the injection plane.

5.4 Numerical results and discussion

In Fig. 11 we plot the spin depolarization length L [panel (a)] and the spin depolarization time τ [panel (b)] as a function of the electric field amplitude, for three values of the lattice temperature. The spin relaxation lengths show a marked maximum that rapidly reduces its intensity, widens and moves towards higher electric field amplitudes with the increasing of the temperature. For temperatures $T \leqslant 150$ K the decoherence times plotted in Fig. 11 (b) show a non-monotonic behavior. For $E_0 > 0.5$ kV/cm, τ lightly depends on the temperature up to $T \sim 150$ K. At higher temperatures, the spin electron relaxation time becomes a monotonic decreasing function of the electric field intensity. The presence of maxima in the spin depolarization length at intermediate fields can be explained by the interplay between two competing factors: in the linear regime, as the field enlarges, the electron momentum and the drift velocity increase in the direction of the field. On the other hand, the increased electron momentum also brings about a stronger effective magnetic field, as shown in Eq. 20 (Barry et al., 2003). Consequently, the electron precession frequency becomes higher, resulting in faster spin relaxation (i.e., shorter spin relaxation time). For $E_0 < 0.5$ kV/cm and $T \leqslant 150$ K the non-monotonic behavior of the relaxation time reflects the complex scenario described above, caused by the triggering of scattering mechanisms having different rates of occurrence.
In Fig. 12 we show the spin electron relaxation length L [panel (a)] and the spin depolarization time τ [panel (b)] as a function of the lattice temperature, for five values of the electric field amplitude. For a fixed electric field, L is a monotonic decreasing function of the temperature. When $E_0 = 0.5$ kV/cm, L shows its maximum value, remaining greater than 35 μm up to $T \simeq$ 80 K. Furthermore, for field amplitudes greater than 1 kV/cm, the spin depolarization length remains almost constant for $T < 100$ K. At room temperature the maximum value of L ($\sim$ 6 μm) is obtained for $E_0 \geqslant 1$ kV/cm. The relaxation time τ shows, instead, a non-monotonic behavior with the temperature [see Fig. 12 (b)]. In particular, the curve obtained with $E_0 =$ 0.1 kV/cm exhibits a minimum at $T \sim 80$ K and an increase in the range $80 - 150$ K. For temperatures greater than 150 K, all curves with a field strength up to 0.5 kV/cm show a common decreasing trend. The longest value of spin coherence time is achieved for the field amplitude $E_0 = 0.5$ kV/cm for the entire range of temperatures. For higher values of E_0, the spin depolarization time strongly decreases, becoming nearly temperature-independent for $E_0 > 1.5$ kV/cm. As the temperature increases, the scattering rate increases too, and hence the ensemble of spins loses its spatial order faster, resulting in a faster spin relaxation. This temperature dependence becomes less evident at higher amplitudes of the driving electric field, where, because of the greater drift velocities, the polarization loss is mainly due the to strong effective magnetic field. At very low electric fields, the spin dephasing is, instead, primarily caused by the multiple scattering events. The nonmonotonicity of τ can be ascribed by the progressive change, with the increase of the temperature, of the dominant collisional mechanism from acoustic phonons and ionized impurities to polar optical phonons (Dzhioev et al., 2004). Following the theory of D'yakonov-Perel, τ^{-1} is proportional to the third power of the temperature T and linearly depends on the momentum relaxation time τ_p (Dyakonov & Perel, 1971). An increase of the temperature initially leads to a slightly decrease of τ; for

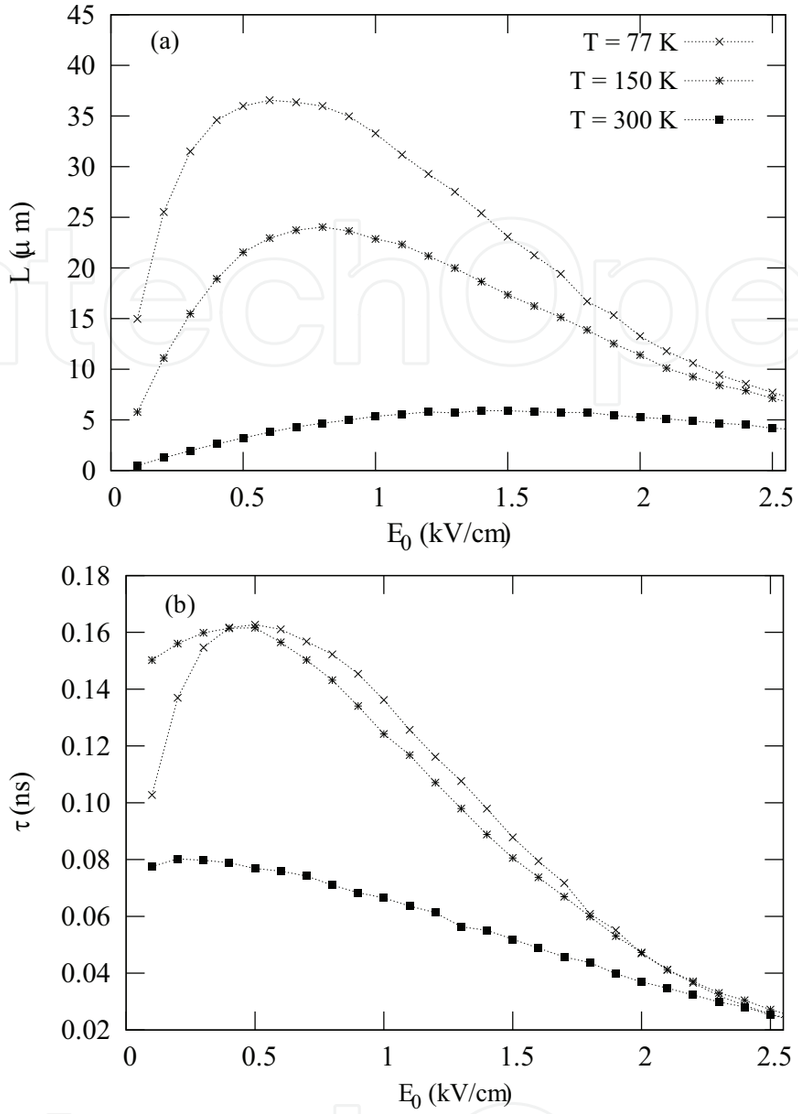

Fig. 11. Spin depolarization length L (a) and spin depolarization time τ (b) as a function of the electric field amplitude E_0, for three values of the lattice temperature T.

temperatures greater than $\sim$ 100 K the electrons start to experience scattering by polar optical phonons. This switching on leads to an abrupt decrease of τ_p that, for lattice temperatures in the range $100 - 150$ K, results more effective than the increase of T, giving rise to the observed increase of τ. For temperatures greater than 150 K this latter effect is no more relevant.

5.5 Conclusions

We have estimated the spin mean lifetimes and depolarization lengths of an ensemble of conduction electrons in lightly doped n-type GaAs crystals, in a wide range of both lattice temperatures ($10 < T < 300$ K) and field intensities ($0.1 < E_0 < 2.5$ kV/cm), finding that, under particular conditions, also at temperatures greater than the liquid-helium temperature, it is possible to obtain very long spin relaxation times and relaxation lengths. These are

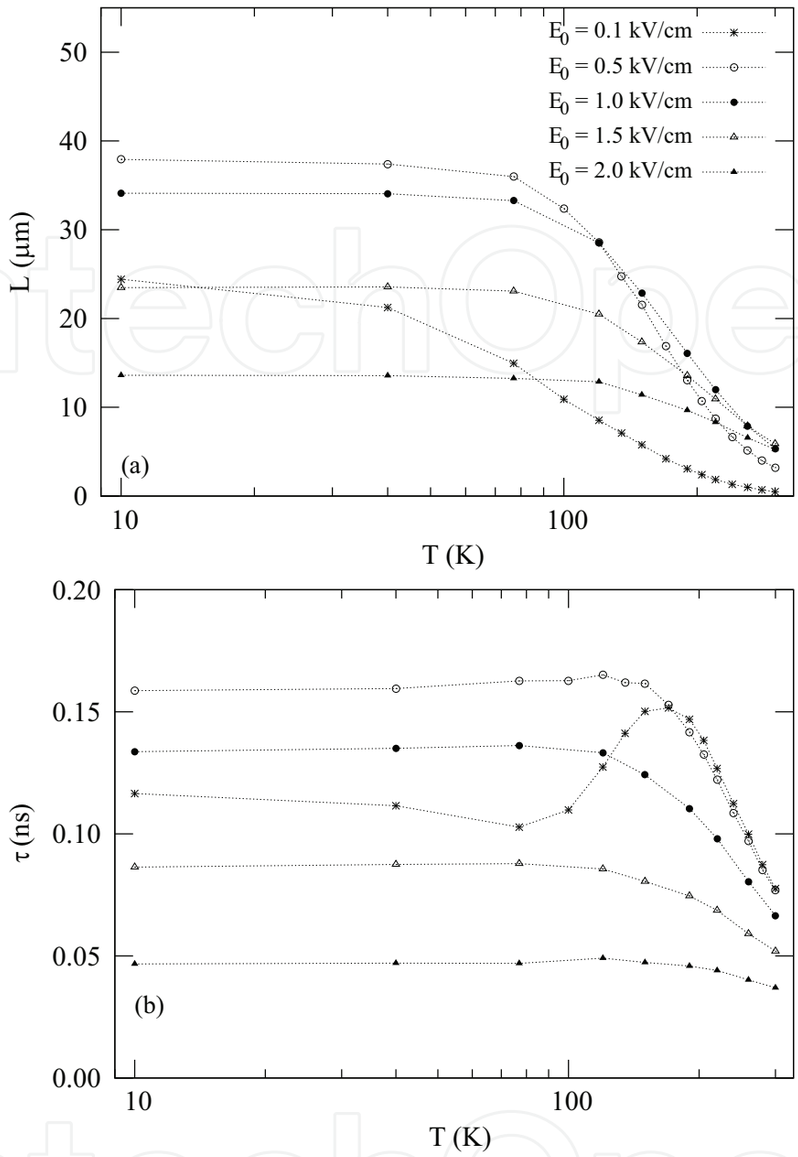

Fig. 12. Spin depolarization length L(a) and spin depolarization time τ (b) as a function of the temperature T, for five values of the electric field amplitude E_0.

essential for the high performance of spin-based devices, in order to extend the functionality of conventional devices to higher working temperatures and higher electric field amplitudes and to allow the development of new information processing systems. In particular, for $E_0 = 0.5$ kV/cm we achieve the longer value of spin lifetime ($\tau > 0.15$ ns) up to a temperature $T = 150$ K. At room temperatures, we obtain a coherence length of about 6 μm, nearly independent from the intensity of the electric field. Furthermore, depending on the interplay between the external electric field and the different collisional mechanisms with increasing electron energy, we find very interesting nonmonotonic behavior of spin lifetimes and depolarization lengths as a function of temperature and electric field amplitude.

6. Acknowledgements

This work was partially supported by MIUR and CNISM-INFM. DPA would like to thank Prof. G. Ferrante, Prof. M. Zarcone, Dr. M.C. Capizzo (Harmonic generation processes), Prof. B. Spagnolo, Dr. N. Pizzolato and Dr. S. Spezia (hot-carrier noise and spin relaxation) for their interesting ideas, helpful discussions and excellent collaborations and, in particular, N. Pizzolato and S. Spezia for the proofreading of the whole manuscript. Moreover, the author is very thankful to Prof. M.W. Wu, who improved the spintronics part with valuable comments and suggestions.

7. References

Abragam, A. (1961) *The Principles of Nuclear Magnetism*, Clarendon Press, Oxford.

Alekseev,K.N.; Erementchouk, M.V. & Kusmartsev, F.V. (1999). Direct current generation due to wave mixing in semiconductors. *Europhys. Lett.*, 47, 595.

Barry, E.A.; Kiselev A.A. & Kim K.W. (2003). Electron spin relaxation under drift in GaAs. *Appl. Phys. Lett.*, 82, 3686.

Beck, M.; Metzner, C.; Malzer, S. & Döhler G.H. (2006). Spin lifetimes and strain-controlled spin precession of drifting electrons in GaAs. *Europhys. Lett.*, 75, 597.

Bir, G.L.; Aronov, A.G. & Pikus, G.E. (1976). Spin relaxation of electrons due to scattering by holes. *Sov. Phys. - JETP* 42, 705

Borca, B.; Flegel, A.V.; Frolov, M.V.; Manakov, N.L.; Milosevic, D.B. & Starace, A.F. (2000). Static-Electric-Field-Induced Polarization Effects in Harmonic Generation. *Phys. Rev. Lett.*, 85, 732.

Bournel, A.; Dollfus, P.; Cassan, E. & Hesto P. (2000). Monte Carlo study of spin relaxation in AlGaAs/GaAs quantum wells. *Appl. Phys. Lett.*,77, 2346.

Brazis, R.; Raguotis, R. & Siegrist, M.R. (1998). Suitability of drift nonlinearity in Si, GaAs, and InP for high-power frequency converters with a 1 THz radiation output. *J. Appl. Phys.*,84, 3474.

Brazis, R.; Raguotis, R.; Moreau, Ph. & Siegrist, M.R. (2000). Enhanced Third-Order Nonlinearity in Semiconductors Giving Rise to 1 THz Radiation. *Int. J. Infrared Millim. Waves*,21, 593.

Dash, S.P.; Sharma, S.; Patel, R.S.; De Jong, M.P. & Jansen, R. (2009). Electrical creation of spin polarization in silicon at room temperature. *Nature* 462, 491.

Dyakonov, M.I. & Perel V.I. (1971). Spin relaxation of conduction electrons in noncentrosymmetric semiconductors. *Sov. Phys. - Solid State*,13, 3023.

Dyakonov, M.I. (2006). Introduction to spin physics in semiconductors. *Physica E*,35, 246.

Dzhioev,R.I.; Kavokin, K.V.; Korenev,V.L.; Lazarev,M.V.; Poletaev, N.K.; Zakharchenya, B.P.; Stinaff, E.A.; Gammon, D.; Bracker, A.S. & Ware, M.E. (2004). Suppression of Dyakonov-Perel Spin Relaxation in High-Mobility n-GaAs. *Phys. Rev. Lett.*, 93, 216402.

Dudovich, N.; Smirnova, O.; Levesque, J.; Mairesse, Y.; Ivanov, M.Yu.; Villeneuve, D.M. & Corkum, P.B.(2006). Measuring and controlling the birth of attosecond XUV pulses. *Nature Physics*, 2, 781.

Elliott, R.J. (1954). Theory of the Effect of Spin-Orbit Coupling on Magnetic Resonance in Some Semiconductors. *Phys. Rev.*,96, 266.

Ferrante, G.; Zarcone, M. & Uryupin, S.A. (2000). Harmonic generation and wave mixing in a plasma in the presence of two linearly polarized laser fields. *J. Opt. Soc. Am. B*,17, 1383.

Ferrante, G.; Zarcone, M. & Uryupin, S.A. (2004a). Plasma radiation spectra in the presence of static electric and high-frequency radiation fields. *Eur. Phys. J. D* ,31, 77.

Ferrante, G.; Zarcone, M. & Uryupin, S.A. (2004b). Laser even harmonics generation by a plasma embedded in a static electric field. *Laser Phys. Lett.*,1, 167.

Ferrante, G.; Zarcone, M. Uryupin, S.A. (2005). Even harmonics generation of high frequency radiation in current-carrying plasmas. *Physics of Plasmas*,12, 052111.

Furis, M.; Smith, D.L.; Crooker, S.A. & Reno, J.L. (2006). Bias-dependent electron spin lifetimes in n-GaAs and the role of donor impact ionization. *Appl. Phys. Lett.*, 89, 102102.

González, T.; Pérez, S.; Starikov, E.; Shiktorov. P.; Gruzinskis, V.; Reggiani, L.; Varani, L. & Vaissiére, J.C. (2003). Microscopic investigation of large-signal noise in semiconductor materials and devices. *Proc. of SPIE*, 5113, p. 252.

Hägele, D.;Oestreich, M.; Rühle, W.W., Nestle, N.; Eberl, K. (1998). Spin transport in GaAs. *Appl. Phys. Lett.*, 73, 1580.

Hruška, M.; Kos, Š.; Crooker, S.A.; Saxena, A.; Smith, D.L. (2006). Effects of strain, electric, and magnetic fields on lateral electron-spin transport in semiconductor epilayers. *Phys. Rev. B*, 73, 075306.

Ivchenko, E.L.; Lyanda-Geller, Y.B. & Pikus, G.E. (1990). Electric current of optically polarized and thermalized carriers. *Sov. Phys.-JEPT*, 71, 550.

Jiang J.H. & Wu M.W. (2009). Electron spin relaxation in bulk III-V semiconductors from a fully microscopic kinetic spin Bloch equation approach. *Phys. Rev. B*, 79, 125206.

Kikkawa, J.M. & Awschalom, D.D. (1998). Resonant Spin Amplification in n-Type GaAs. *Phys. Rev. Lett.*, 80, 4313.

Kiselev, A.A. & Kim, K.W. (2000). Progressive suppression of spin relaxation in two-dimensional channels of finite width. *Phys. Rev. B*,61, 13115.

Litvinenko, K. L.; Leontiadou, M.A.; Li, J.; Clowes, S.K.; Emeny, M. T.; Ashley, T.; Pidgeon, C.R.; Cohen, L.F. & Murdin, B.N. (2010). Strong dependence of spin dynamics on the orientation of an external magnetic field for InSb and InAs. *Appl. Phys. Lett.*, 96, 111107.

Mairesse,Y.; Haessler,S.; Fabre, B.; Higuet, J.; Boutu,W.; Breger,P.; Constant, E.; Descamps, D.; Mével, E.; Petit, S. & Salières, P. (2008). Polarization-resolved pump probe spectroscopy with high harmonics. *New J. Phys.*, 10 , 025028.

Mikhailov S.A. (2008). Electromagnetic response of electrons in graphene: Non-linear effects. *Physica E: Low-dimensional Systems and Nanostructures*,40, 2626.

Mikhailov S.A.(2009). Non-linear graphene optics for terahertz applications. *Microelectronics Journal*,40, 712.

Mishchenko, E.G. & Halperin, B.I. (2003).Transport equations for a two-dimensional electron gas with spin-orbit interaction. *Phys. Rev. B*,68, 045317.

Moreau,Ph.; Siegrist, M.R.; Brazis, R. & Raguotis R. (1999). Enhancement of the Third Harmonic Generation Efficiency in n-Type Si and InP by Cooling from Room Temperature to 80 K. *Mat. Science Forum* ,297-298, 315.

Paget, D.; Lampel, G.; Sapoval, B. & Safarov V.I. (1977).Low field electron-nuclear spin coupling in gallium arsenide under optical pumping conditions. *Phys. Rev. B*,15, 5780.

Perry, M. & Krane, J.(1993). High-order harmonic emission from mixed fields. *Phys. Rev. A*,48, R4051.

Nougier, J.P. (1994). Fluctuations and noise of hot carriers in semiconductor materials and devices. *IEEE Trans. Electr. Dev.*, 41, 2034.

Persano Adorno, D.; Zarcone, M.& Ferrante, G. (2000). Far-Infrared Harmonic Generation in Semiconductors. A Monte Carlo Simulation. *Laser Physics*, 10, 310.

Persano Adorno, D.; Zarcone, M.& Ferrante, G. (2001). Monte Carlo Simulation of Harmonic Generation in InP. *Laser Part. Beams*,19, 81.

Persano Adorno, D.; Zarcone, M.& Ferrante, G. (2003a). High-Order Harmonic Emission from Mixed Fields in n-type low-doped Silicon. *Laser Physics*,13, 270.

Persano Adorno, D.; Zarcone, M.& Ferrante, G. (2003b). High harmonic generation by two color field-mixing in n-type low-doped GaAs. *Phys. Status Solidi C* ,0, 1488.

Persano Adorno, D.; Zarcone, M.; Ferrante, G.; Shiktorov, P.; Starikov, E.; Gruzinskis, V.; Perez, S.; Gonzalez, T.; Reggiani, L.; Varani, L. & Vaissiere, J.C. (2004).Monte Carlo Simulation of high-order harmonics generation in bulk semiconductors and submicron structures. *Phys. Stat. Sol. C* ,1, 1367.

Persano Adorno, D.; Capizzo, M.C. & Zarcone, M. (2007a).Monte Carlo Simulation of Harmonic Generation in GaAs structures operating under large-signal Conditions. *J. Comput. Electron.*,6, 27.

Persano Adorno, D.; Zarcone, M.& Ferrante, G. (2007b). Generation of even harmonics of sub-THz radiation in bulk GaAs in the presence of a static electric field. *J. Comput. Electron.*,6, 31.

Persano Adorno, D.; Capizzo, M.C. & Zarcone, M. (2008a). Changes of electronic noise induced by oscillating fields in bulk GaAs semiconductors. *Fluct. Noise Lett.*, 8, L11.

Persano Adorno, D.; Pizzolato, N. & Spagnolo, B. (2008b). External noise effects on the electron velocity fluctuations in semiconductors. *Acta Phys. Pol.* A, 113, 985.

Persano Adorno, D.; Pizzolato, N.& Spagnolo, B. (2009a). Noise influence on electron dynamics in semiconductors driven by a periodic electric field. *Journal of Statistical Mechanics: Theory and Experiment* , P01039-10.

Persano Adorno, D.; Pizzolato, N.& Spagnolo, B. (2009b). Monte Carlo Study of Diffusion Noise Reduction in GaAs Operating under Periodic Conditions. *CP1129, Noise and Fluctuations, Proc. of the 20th International Conference (ICNF 2009)*, edited by M. Macucci and G. Basso,(American Institute of Physics) p 121.

Persano Adorno, D.(2010). Polarization of the Radiation Emitted in GaAs Semiconductors Driven by Far-Infrared Fields *Laser Physics*, 20, 1061.

Pershin, Y. (2005). Long-lived spin coherence states in semiconductor heterostructures. *Phys. Rev. B*,71, 155317.

Pikus, G.E & Titkov, A.N. (1989) *Optical Orientation*, edited by Meyer F., Nauka (Leningrad).

Pramanik, S.; Bandyopadhyay, S. & Cahay, M. (2003).Spin dephasing in quantum wires. *Phys. Rev. B*, 68, 075313.

Romanov, Yu A.; Romanova, J. Yu; Mourokh, L.G. & Horing, N.J.M. (2004). Nonlinear properties of semiconductor superlattices in a biharmonic field. *Semicond. Sci. Technol.*,19, S80.

Saikin, S.; Shen, M.; Cheng, M.C. & Privman, V. (2003). Semiclassical Monte Carlo model for in-plane transport of spin-polarized electrons in III V heterostructures. *J. Appl. Phys.*,94, 1769.

Saikin, S. (2004). A drift-diffusion model for spin-polarized transport in a two-dimensional non-degenerate electron gas controlled by spin orbit interaction. *J. Phys.: Condens. Matter*, 16, 5071.

Saikin, S.; Shen, M. & Cheng, M.C. (2006). Spin dynamics in a compound semiconductor spintronic structure with a Schottky barrier. *J. Phys.: Condens. Matter*, 18, 1535.

Sanada,H.; Arata, I.; Ohno, Y.; Chen, Z.; Kayanuma,K.; Oka, Y.; Matsukura, F. & Ohno H.(2002). Relaxation of photoinjected spins during drift transport in GaAs. *Appl. Phys. Lett.*, 81, 2788.

Shen, M.; Saikin, S.; Cheng, M.C. & Privman, V. (2004). Monte Carlo Modeling of Spin FETs Controlled by Spin-Orbit Interaction. *Mathematics and Computers in Simulation*, 65, 351.

Shiktorov, P.; Starikov, E.; Gruzinskis, V.; Zarcone, M.; Persano Adorno, D.; Ferrante, G., (b), Reggiani, L.; Varani, L. & Vaissiére, J.C. (2002a). Monte Carlo Analysis of the Efficiency of Tera-Hertz Harmonic Generation in Semiconductor Nitrides. *Phys. stat. sol. (a)* ,190, 271.

Shiktorov, P.; Starikov, E.; Gruzinskis, V.; Reggiani, L.; Varani, L. & Vaissiére, J.C. (2002b). Monte Carlo calculation of electronic noise under high-order harmonic generation. *Appl. Phys. Lett.*, 80, 4759.

Shiktorov, P.; Starikov, E.; Gruzinskis, V.; Perez, S.; Gonzalez, T.; Reggiani, L.; Varani, L. & Vaissiere, J.C.(2003a). Monte Carlo simulation of threshold bandwidth for high-order harmonic extraction. *IEEE Trans. Electr. Dev.*, 50, 1171.

Shiktorov, P.; Starikov, E.; Gruzinskis, V.; Pérez, S.; González, T.; Reggiani, L.; Varani, L. & Vaissiére, J.C. (2003b). Upconversion of partition noise in semiconductors operating under periodic large-signal conditions. *Phys. Rev. B* , 67 165201.

Song,X.; Gong, S.; Jin, S. & Xu Z.(2003). Two-color interference effects for ultrashort laser pulses propagating in a two-level medium. *Physics Letters A*, 319, 150.

Spezia, S.; Persano Adorno, D.; Pizzolato, N.& Spagnolo, B. (2010). Temperature Dependence of Spin Depolarization of Drifting Electrons in n-type GaAs Bulks. *Acta Phys. Pol.* B, 41, 1171.

Spezia, S.; Persano Adorno, D.; Pizzolato, N.& Spagnolo, B. (in press). Doping dependence of spin dynamics of drifting electrons in GaAs bulks. *Acta Phys. Pol.* A.

Urban, M.; Nieswand, Ch.; Siegrist, M.R. & Keilmann,F. (1995). Intensity dependence of the third-harmonic-generation efficiency for high-power far-infrared radiation in n-silicon. *J. Appl. Phys.*,77, 981.

Urban, M.; Siegrist, M.R.; Asadauskas, L.; Raguotis, R. & Brazis,R. (1996). A precise new method to evaluate Monte Carlo simulations of electron transport in semiconductors. *Appl. Phys. Lett.*,69, 1776.

Varani, L.; Palermo, C.; De Vasconcelos, C.; Millithaler, J.F.; Vaissiére, J.C.; Nougier, J.P.; Starikov, E.; Shiktorov, P. & Gruzinskis, V. (2005). Is It Possible To Suppress Noise By Noise In Semiconductors? *Proc.Int. Conf. on Unsolved Problems of Noise and Fluctuations*(American Institute of Physics) p 474.

Vilar, J.M.G. & Rubí, J.M. (2001). Noise Suppression by Noise. *Phys. Rev. Lett.*, 86, 950.

Walton, D.B. & Visscher, K. (2004). Noise suppression and spectral decomposition for state-dependent noise in the presence of a stationary fluctuating input. *Phys. Rev.* E, 69 051110-1.

Wang, B.; Li, X. & Fu,P.(1999). Polarization effects in high-harmonic generation in the presence of static-electric field. *Phys. Rev. A*, 59, 2894.

Weng, M.Q. & Wu, M.W. (2003). Kinetic theory of spin transport in n-type semiconductor quantum wells. *J. Appl. Phys.*, 93, 410.

Weng, M.Q.; Wu, M.W. & Jiang, L. (2004). Hot-electron effect in spin dephasing in n-type GaAs quantum wells. *Phys. Rew. B*, 69, 245320.

Wu, M.W. & Ning, C.Z. (2000). Dyakonov-Perel Effect on Spin Dephasing in n-Type GaAs. *Phys. Status Solidi B*, 222, 523.

Wu, M.W.; Jiang, J.H. & Weng, M.Q. (2010). Spin dynamics in semiconductors. *Physics Reports*, 493, 61.

Xia,K.; Niua, Y.; Li C. & Gong, S. (2007). Absolute phase control of spectra effects in a two-level medium driven by two-color ultrashort laser pulses. *Physics Letters A*, 361, 173.

Yafet, Y. (1963) *Solid State Physics*, edited by F. Seitz and D. Turnbull, (New York) Academic, Vol. 14, p. 2.

Zhang, P.; Zhou, J. & Wu, M.W. (2008). Multivalley spin relaxation in the presence of high in-plane electric fields in n-type GaAs quantum wells. *Phys. Rev. B*, 77, 235323.

Applications of Monte Carlo Method in Science and Engineering
Edited by Prof. Shaul Mordechai

ISBN 978-953-307-691-1
Hard cover, 950 pages
Publisher InTech
Published online 28, February, 2011
Published in print edition February, 2011

In this book, Applications of Monte Carlo Method in Science and Engineering, we further expose the broad range of applications of Monte Carlo simulation in the fields of Quantum Physics, Statistical Physics, Reliability, Medical Physics, Polycrystalline Materials, Ising Model, Chemistry, Agriculture, Food Processing, X-ray Imaging, Electron Dynamics in Doped Semiconductors, Metallurgy, Remote Sensing and much more diverse topics. The book chapters included in this volume clearly reflect the current scientific importance of Monte Carlo techniques in various fields of research.

InTech Europe
University Campus STeP Ri
Slavka Krautzeka 83/A
51000 Rijeka, Croatia
Phone: +385 (51) 770 447
Fax: +385 (51) 686 166
www.intechopen.com

InTech China
Unit 405, Office Block, Hotel Equatorial Shanghai
No.65, Yan An Road (West), Shanghai, 200040, China
中国上海市延安西路65号上海国际贵都大饭店办公楼405单元
Phone: +86-21-62489820
Fax: +86-21-62489821

IntechOpen